



King's Research Portal

DOI:

[10.1016/j.compbimed.2018.07.008](https://doi.org/10.1016/j.compbimed.2018.07.008)

Document Version

Peer reviewed version

[Link to publication record in King's Research Portal](#)

Citation for published version (APA):

Handa, B. S., Roney, C. H., Houston, C., Qureshi, N. A., Li, X., Pitcher, D. S., Chowdhury, R. A., Lim, P. B., Dupont, E., Niederer, S. A., Cantwell, C. D., Peters, N. S., & Ng, F. S. (2018). Analytical approaches for myocardial fibrillation signals. *Computers in Biology and Medicine*.
<https://doi.org/10.1016/j.compbimed.2018.07.008>

Citing this paper

Please note that where the full-text provided on King's Research Portal is the Author Accepted Manuscript or Post-Print version this may differ from the final Published version. If citing, it is advised that you check and use the publisher's definitive version for pagination, volume/issue, and date of publication details. And where the final published version is provided on the Research Portal, if citing you are again advised to check the publisher's website for any subsequent corrections.

General rights

Copyright and moral rights for the publications made accessible in the Research Portal are retained by the authors and/or other copyright owners and it is a condition of accessing publications that users recognize and abide by the legal requirements associated with these rights.

- Users may download and print one copy of any publication from the Research Portal for the purpose of private study or research.
- You may not further distribute the material or use it for any profit-making activity or commercial gain
- You may freely distribute the URL identifying the publication in the Research Portal

Take down policy

If you believe that this document breaches copyright please contact librarypure@kcl.ac.uk providing details, and we will remove access to the work immediately and investigate your claim.

Analytical Approaches for Myocardial Fibrillation Signals

Balvinder S Handa, BSc, MRCP¹, Caroline Roney, PhD³, Charles Houston, MRes¹, Norman Qureshi, MRCP, PhD¹, Xinyang Li, PhD¹, David Pitcher, PhD¹, Rasheda A Chowdhury, PhD¹, Phang Boon Lim, MRCP, PhD¹, Emmanuel Dupont, PhD¹, Steven Niederer, PhD³, Chris Cantwell, PhD², Nicholas S. Peters, FRCP, MD¹, Fu Siong Ng, MRCP, PhD¹.

¹ National Heart & Lung Institute, Imperial College London, United Kingdom

² Department of Aeronautics, Imperial College London, United Kingdom

³ King's College London, United Kingdom

Correspondence to:

Dr Fu Siong Ng

4th Floor, Imperial Centre for Translational and Experimental Medicine,

Imperial College London, Hammersmith Campus,

Du Cane Road, London W12 0NN,

United Kingdom.

E-mail: f.ng@imperial.ac.uk

Tel: +442075943614

Abstract

Atrial and ventricular fibrillation are complex arrhythmias, and their underlying mechanisms remain widely debated and incompletely understood. This is partly because the electrical signals recorded during myocardial fibrillation are themselves complex and difficult to interpret with simple analytical tools. There are currently a number of analytical approaches to handle fibrillation data. Some of these techniques focus on mapping putative drivers of myocardial fibrillation, such as dominant frequency, organizational index, Shannon entropy and phase mapping. Other techniques focus on mapping the underlying myocardial substrate sustaining fibrillation, such as voltage mapping and complex fractionated electrogram mapping. In this review, we discuss these techniques, their application and their limitations, with reference to our experimental and clinical data. We also describe novel tools including a new algorithm to map microreentrant circuits sustaining fibrillation.

Key words: atrial fibrillation, ventricular fibrillation, analysis, voltage mapping, rotors, phase analysis, shannon entropy, dominant frequency, organizational index, complex fractionated electrograms

1. Introduction

Atrial fibrillation (AF) and ventricular fibrillation (VF) are complex arrhythmias, and the electrophysiological mechanisms that underlie these arrhythmias are still incompletely understood. For both AF and VF, there is debate as to whether these arrhythmias are entirely disorganized rhythms, sustained by multiple wavefronts, or if they are sustained by an organized driver with fibrillatory conduction distant from the driver (1). The ongoing uncertainty about the mechanisms of myocardial fibrillation is in part due to the limitations of currently available tools used to record fibrillatory data, such as limits in resolution, but is also largely due to the challenges in processing and interpreting the complex signals seen in myocardial fibrillation.

The commonly used methods to record signals during myocardial fibrillation in the experimental electrophysiology laboratory include recording electrograms using contact electrodes (2), or recording optical signals non-invasively in preparations loaded with potentiometric dyes (3). In the clinical electrophysiology laboratory, contact electrogram recordings are most commonly used (4), although non-contact electrograms can also be recorded, aided by inverse solution mathematics (5).

Because of the complex nature of myocardial fibrillation, these recorded electrical or optical signals often appear chaotic, and the periodicity and organisation within the signal can be difficult to appreciate from the raw data. The challenge of any analytical approach used to handle fibrillatory data is to accurately translate what appear to be chaotic and disorganized

signals into interpretable information about the nature of the propagating wavefronts and the underlying myocardial substrate sustaining the fibrillation.

In this review, we will first briefly summarize our current understanding of the mechanisms of AF and VF. We will then describe in detail, the utility and application of a number of analytical techniques used to process myocardial fibrillation data, including commonly used techniques such as dominant frequency (DF) analysis, Shannon entropy (SE), phase mapping, voltage and complex fractionated atrial electrogram mapping, illustrating these techniques with our own experimental and clinical data. In addition, we will also describe novel analytical tools developed in our laboratory, including methods for identifying lines of conduction block in cases where fibrillation is sustained by microreentrant circuits.

2. Current understanding of mechanisms of myocardial fibrillation

2.1 Atrial fibrillation

Our understanding of AF mechanisms has evolved over time. In the early 1900s, a “single focus” theory was proposed, whereby a rapidly firing single focus was postulated to produce atrial flutter or AF depending on the rate (6). Thereafter, Moe *et al* in 1960s, using a computer model of impulse propagation in a non-uniform two dimensional structure, described AF as being sustained by random self-perpetuating multiple wavelets throughout atrial tissue (7). A study by Allessie *et al.* provided first experimental evidence of the multiple wavelet hypothesis showing that the coexistence of 4 to 6 wavelets was necessary for maintaining AF perpetuation in a canine heart model (8). However, no rigorous proof exists to support the theory that a critical number of wavelets are required to maintain fibrillation.

The contrary hierarchical hypothesis was supported by work by Jalife *et al* in the 1990s that stated AF was sustained by highly organized drivers in the form of spiral waves or rotors that self-perpetuated through wavefront and wavetail interactions at a phase singularity point, without a need for an anatomical obstacle (9). A phase singularity point resides at the core of a rotor and represents an area without a definite phase surrounded by neighbouring areas that show continuous cycling between $-\pi$ to $+\pi$ in a time and space dependent signal (1). More recently, there has been increasing interest in the endo-epicardial dissociation hypothesis, which proposes that complex fibrillation is sustained by electrical dissociation of the different layers of myocardial tissue in the atrium, allowing waves to break through from one layer to another, increasing the complexity of fibrillation and the effective area through which it propagates (10).

2.2 Ventricular fibrillation

There is a paucity of data on VF mechanisms in human due to its short-lived and lethal nature. Our understanding of mechanisms involved in its genesis and perpetuation remain incomplete and is largely based on animal experiments or extrapolation from mechanisms described in AF. Moe's original multiple wavelet theory of AF was also found to be applicable in VF in some earlier studies (11). VF has frequently been described as a form of spatio-temporal chaos with 'quasiperiodic transition to chaos' whereby an initial primary spiral wave or re-entrant driver degenerates to a period of alternans and finally complete chaos (12). In patients undergoing cardiac surgery this theory has been demonstrated to some extent. VF induced on cardiopulmonary bypass has been and shown to demonstrate a degree of spatiotemporal organization at onset that degenerates and becomes more disorganized as it evolves (13). The contrary hypothesis that VF is an organized phenomenon is also supported

by some data in the literature. Organized drivers in non-ischaemic myocardial tissue and disorganized activation in ischaemic and border zone area have been described in animal models (2),(14). Spiral wave rotational drivers have also been shown in *in silico* models and hypothesised to be the primary driver (15). Intramural re-entry has been described in *ex vivo* perfused human hearts at sites of fibrosis (16), whilst mapping with basket catheters has demonstrated spiral wave re-entry during VF induction in ventricular tachycardia ablation procedures (17).

3. Approaches to mapping sources of myocardial fibrillation

3.1 Dominant Frequency

Fibrillation data, whether recorded directly as voltage readings by contact electrograms or indirectly by fluorescence on optical mapping is a time series of a changing signal. The hypothesis is that, in complex fibrillatory signals, which lack clearly identifiable cycle lengths due to constant amplitude and frequency changes, the areas with the highest dominant frequencies represent areas that are driving the fibrillation, and by abolishing it, the process can be terminated (18).

The dominant frequency of a signal is defined as the frequency with highest energy in the power spectrum. Practically, the discretely sampled time-domain signal is transformed into the frequency domain using a discrete Fourier transform (or fast Fourier transform) and the relative power of each frequency is calculated. For a spectrum $X(f)$, the dominant frequency is defined as the frequency of highest amplitude, i.e.,

$$DF = \arg \max_f X(f)$$

3.1.1 Dominant frequency and rotational drivers

Sites of high DF compared to their surroundings have been postulated to be sites of primary activation and localise to areas identified as sustaining rotational activity in fibrillation (19), (20). Simulation studies of stable long duration rotors termed ‘mother rotors’ have demonstrated highest DF values at the core (21). [Figure 1A and 1B](#) demonstrate an example of a DF map in rat VF. The frequency spectrum of the optical signal at each pixel was calculated. The frequency with the greatest power was designated as the DF of that pixel and a DF map was created. In this example, there was a spectrum of frequencies between 10 to 27 Hz with a DF of 26Hz. The highest or maximal DF in this example occupied a large spatial area rather than a discrete point that identified a primary activation site.

3.1.2 Dominant frequency in clinical experience

Electrograms have been used to construct DF maps of the atrium, with areas of maximal DF subsequently targeted for ablation. In a randomised control trial designed to assess the effectiveness of targeting high- (dominant) frequency source ablation (HFSA) in AF, this approach was not superior to conventional treatment (22). However, global DF measures, such as an overall reduction in the maximal DF, have been associated with reduced AF recurrence and abolishing baseline LA to right atrium (RA) DF gradients that often exist in AF with ablation has been associated with long term maintenance of sinus rhythm (23). In our rat VF experiments, whilst we observed higher relative DF values in areas of rotational

drivers, areas with high DF were also seen at areas without drivers, suggesting limited specificity of DF mapping for fibrillatory drivers.

3.2 Organizational Index

DF maps in AF have been found to be spatiotemporally unstable and ‘high’ DF values spuriously result from wave front collision in areas remote from rotational activity, calling into question feasibility of DF guided ablation. Our group has previously postulated that sites with high DF organization, termed the organizational index (OI), defined as mean ratio of the power of the DF and its harmonics (within a 0.75Hz window) to the total power of the spectrum, may be sites of AF drivers.

In persistent AF (PsAF) patients, ablation of sites of high OI resulted in an increase in the OI of areas remote from these sites (left atrial appendage), supporting the focal source hypothesis (24). Areas of high PS clustering were found to correlate with areas of high OI and there was an increase in OI after circumferential pulmonary vein isolation (PVI) (25). Although interest in DF guided ablation has waned, there might be a role in utilising it with a more spatiotemporally stable methodology such as OI to identify substrate.

3.3 Shannon Entropy

Entropy is a measure of unpredictability of information content. Shannon entropy (SE) is a measure that calculates the smallest number of bits to communicate an amount of information losslessly. Signals that are predictable, for instance, sinus rhythm on an ECG, have low arbitrary entropy values whereas those that are more variable such as VF on ECG would have high entropy values (26). SE can be applied to electrogram or optical mapping data from

different spatial locations within a ventricle or atrium to construct SE maps and by discerning areas of high and low entropy, driver regions may be identified. SE is calculated by binning the signal using a predefined bin size that is amplitude dependent. The value of SE for signal is then calculated using the relative probability (P_i) of the signal falling in each amplitude bin (N). The equation applied to an electrogram is:

$$SE = \sum_{i=1}^{N-1} P_i \cdot \log_2 P_i$$

3.3.1 Shannon entropy and rotational drivers

The primary objective of applying SE to fibrillation data is to identify rotational activity or drivers either from its value in a single area relative to others, or from calculation of a SE gradient (26). In animal AF and VF models, SE has been applied to optical mapping signals to show a gradient in values with higher SE values occurring at the core of the rotational activity relative to the surrounding regions. The pivot zone at the core has a more complex fragmented signal with high SE values, whereas further from the core, activation is more regular and periodic with lower SE values. Ganesan *et al* showed this inverse correlation between SE and increasing distance from the pivot point / rotational core using paired optical mapping and bipolar electrogram data in isolated rat and sheep atrial preparations (27). Other animal studies have shown a similar gradient but with a contradicting relationship with a low SE at the core of rotational activity (26),(28). **Figure 2** demonstrates an example of a SE map for our rat model of VF using the method described above. In our experience, when applied to optical mapping data, SE is not able to accurately localise rotational driver regions identified with phase analysis.

3.3.2 Shannon entropy in clinical experience

There is a paucity of SE processed human AF data and its use remains in its infancy. Limited mapping studies have shown areas of high SE outside pulmonary veins in PsAF (28). Only recently, has the feasibility of using SE and other forms of entropy analysis (Renyi and Multiscale Entropy) with 3D LA mapping of AF been explored to identify the potential substrate for ablation (26).

3.4.Phase mapping

Phase mapping is a technique for localizing phase singularities that exist at the core of a rotational driver (29). Over the last two decades, there has been a lot of interest in the hypothesis that ablating tissue in areas that localise phase singularities might be the critical step in treating fibrillation. Some initial clinical studies have shown favorable results for long term freedom from AF with rotor-guided ablation (30), though many subsequent studies have shown disappointing results (31),(32),(33).

3.4.1 Identifying spatiotemporal organization with phase analysis

Despite fibrillation being a seemingly random process, Gray *et al* developed a technique to identify a degree of temporal organization and periodicity in fibrillatory signals (34). They used a technique from nonlinear dynamics called state-space mapping, in which the original signal (the first state variable) is plotted against a time-delayed version of the signal (the second state variable). If there is a consistent dependence of the future samples of the signal on past samples, this will manifest as loops around a central attractor in the coordinate system defined by the two state variables (35). The phase angle then describes the angle as the system moves through this loop or trajectory. This phase angle is measured at each spatial

and temporal location to give a spatial phase map, and a spatial singularity in phase occurs at the center of rotating waves. This landmark paper revealed a degree of spatiotemporal organization in fibrillation and the technique used to reveal this organization is one method that can be used to locate the tip of spiral waves and analyze their dynamics.

3.4.2 Current techniques for phase analysis

Current measurement techniques record a single variable, typically either the extracellular potential or membrane action potential. The phase angle requires the choice of an appropriate second variable. Early studies utilising phase mapping plotted the optical mapping fluorescence signal (used as a surrogate for the membrane potential) against a time shifted fluorescence signal (34). Whereas a particular membrane potential could refer to either depolarization or repolarization, the phase angle gives a unique value for each point in the action potential (36). Phase has the additional advantage that the great variability, present during arrhythmia, in action potential duration and cycle length, does not affect the state-space map (37). Each action potential results in the phase angle preceding through a 2π trajectory, and subthreshold stimuli do not result in loops in the state-space, so long as the time shift and origin of the map are chosen correctly.

There is no consensus on the optimal way to choose an appropriate time shift to generate the second variable: too large a time shift results in overlapping state-space trajectories, while too small a shift means the signals are too similar (34),(38). Another choice of second state variable is the derivative of the first signal, which does not require the choice of a time delay, but is sensitive to noise (39). More recent studies use the Hilbert transform, which is widely used in signal processing, to generate a suitable phase-shifted second variable for phase

analysis (40). **Figure 3** demonstrates an example of phase analysis in a rat model of VF using Hilbert transform, where over a 4 seconds recording, we were able to generate a heat map of tracked phase singularities, which localized to a discrete area near the base of the left ventricle.

A second challenge associated with phase mapping is that phase loops in the two variable phase space should progress around a central point from which the phase angle is calculated. Various techniques have been employed to generate a zero mean signal so that phase loops encircle the origin of the two variable phase space. For example, Bray and Wikswo developed a pseudo-empirical mode decomposition technique in which a line calculated as the mean of maxima and minima splines is removed from the signal to produce a zero mean signal (37). They used a moving window for assigning maxima and minima of a length equal to half of the average cycle length, with the motivation of detecting double potentials that may occur during reentry. Linear and quadratic detrending techniques have also been employed to generate zero mean signals (41),(42).

Spatial maps of phase may be processed to identify phase singularities at which there is a 2π progression in phase in the surrounding points and the phase value is undefined (43). Phase singularities may indicate rotational activity, wavefront break-up or conduction block (44). Analyzing the locations of phase singularities over time is one technique that can be used to reveal the path of rotational activity. Topological rules enforce that the ends of wavefronts must either be connected to each other to form loops, to boundaries or to phase singularities (42).

3.4.3 Application of phase mapping

Phase mapping was originally applied to transmembrane potential data. More recently, techniques have been developed for phase mapping of unipolar and bipolar electrogram data, during both VF (41) and AF (40),(45),(46)(47). The correct calculation of electrogram phase during AF is difficult due to several factors, including the non-sinusoidal and fractionated nature of the electrograms, and the direction-dependency of bipolar electrograms. Kuklik *et al* developed a phase mapping technique using sinusoidal recomposition for atrial unipolar electrograms in which the signal is represented as a sum of sinusoidal wavelets with amplitude proportional to the negative slope of the electrogram (40). This pre-processing generates a sinusoidal signal suitable for phase mapping using the Hilbert Transform. We previously applied a sequence of filters typically used for DF analysis to either bipolar electrograms or the derivative of unipolar electrograms to make the signal more sinusoidal, together with a pseudo-empirical mode decomposition technique to create a zero mean signal, before application of the Hilbert Transform (46). Phase mapping may also be applied to noninvasively computed unipolar electrograms. The filter settings used prior to phase mapping will affect rotor detection (46),(47).

Phase mapping does not assign particular importance to an activation point, which is advantageous for fractionated signals in which it is difficult to assign an activation time. Kuklik *et al* compared cycle lengths calculated from times assigned to the unipolar signals to those calculated from the times of phase inversions and showed a good correlation (40).

Figure 4 shows our methodology for filtering and processing raw unipolar electrograms to calculate phase to track phase singularities. Using data from clinical multipolar catheters and

electroanatomical mapping we are able to generate 3D reconstruction of the left atrium with regions of phase singularities super imposed (**Figure 5**). The number of mapped phase singularities vary between different area of the left atrium and between patients. In our experience, both unipolar and bipolar electrograms are similarly effective in their ability to track phase singularities from clinical data sets (46).

3.4.4 Impact of spatial resolution on phase analysis

Recording modalities are typically limited in either resolution or coverage. We recently investigated how spatial resolution affects interpretation of AF recordings, expressing spatial resolution requirements as a linear function of the spatial wavelength, and found that high-density multipolar catheters provide sufficient resolution, but basket catheters are prone to false rotor detections (50). Aronis *et al* considered the effects of multiple co-existing rotors on resolution requirements in an *in silico* study and found that including more than one rotor increased errors 10-fold, suggesting higher resolution requirements for cases with multiple sources (51). Jacquemet used a statistical model to investigate the effects of interelectrode spacing and rotor number and showed an increase in false positive and false negative phase singularity detections with increasing interelectrode distance (52).

Phase mapping is a technique that is effective with the high spatiotemporal resolution of laboratory-based technique such as optical mapping, however with the limitations imposed by resolution and coverage of current clinical catheters, it is unsurprising that at present rotor guided ablation as an adjunct to conventional PVI has not been proven to be beneficial in a recent systematic review of 11 separate studies (53).

4. Approaches for mapping the fibrillatory substrate

As opposed to directly mapping the location of putative drivers of myocardial fibrillation, as described above, techniques exist to map the myocardial substrate sustaining fibrillation, which provides additional useful information.

4.1 AF voltage mapping and fibrosis

Voltage amplitude from contact electrograms is often used as a surrogate marker for scar, largely from data extrapolated from mapping in the ventricles, and in identifying diseased myocardium as part of a substrate based approach in catheter ablation of ventricular tachycardia (54). In the clinical cardiac electrophysiology laboratory, attempts have been made to identify and target the anatomical substrate of fibrosis using electrogram voltage mapping. There is evidence to support the hypothesis that the presence and extent of low voltage areas can predict the outcomes of catheter ablation of AF (55). Low-voltage areas in the atrium may represent regions of slow conduction as a manifestation of underlying fibrosis, and/or wave collisions representing more functional electrophysiological change and these regions have been purported to be crucial in the maintenance of AF. Slow conduction in diseased myocardium may be necessary for sustaining rotor activity, and localized rotational activity observed with multipolar endocardial mapping was found to co-localise with regions with very low voltages in AF ($<0.1\text{mV}$) (56).

4.1.1 Electroanatomical voltage mapping

Voltage maps are constructed in the clinical catheter laboratory using three dimensional (3D) electroanatomical mapping (EAM) systems. Contemporary EAM systems construct 3D shells of the cardiac chamber of interest by plotting 'electrical points' as they are sampled from the

endocardial wall by a mapping catheter with an inbuilt sensor which is tracked in space with either a weak magnetic or electrical field. EAM systems depict voltage maps on these 3D reconstruction models as colour coded regions of dense scar, border zone and healthy tissue using voltage amplitude cut offs of $<0.5\text{mV}$, $\leq 0.5-1.5\text{mV}$ and $>1.5\text{mV}$ respectively, for the ventricles (57). The voltage amplitude is measured typically as the potential difference between the peak negative and peak positive deflection (peak to peak) of a bipolar or unipolar electrogram over a defined time window (58). Voltage maps can be created in sinus rhythm, paced rhythm or in AF. One of the challenges of creating voltage maps in fibrillation is that, due to complex nature of the electrograms, it can be difficult to identify the peak to peak deflections accurately and also voltage amplitude can change continuously in fibrillation and vary significantly in sinus rhythm from AF in the same region (59). These observation in fibrillation are hypothesized to be due to cancellation of colliding wavefronts, functional/ anatomical blocks (60) and varying wavefront curvature interaction with bipolar electrodes (61).

4.1.2 Ablation of low voltage regions

Current substrate modification strategies targeting potential sites AF drivers involve targeting these low voltage regions. The spatio-temporal variability of voltage signals in AF underlies the challenges of voltage mapping in AF, and some have adopted an approach of mapping in sinus rhythm or during pacing to more accurately study the underlying substrate. Low voltage areas are more represented in persistent AF than in paroxysmal AF, in studies utilising voltage in the paced-rhythm (62), and in AF(63).

The notion of scar homogenization, once again, extrapolated from catheter ablation of ventricular tachycardia, where multiple ablation lesions are created within myocardial scar to eradicate all potential channels that support the arrhythmia (64) has now been described as part of a substrate modification approach in AF. Rolf *et al* described a novel individualized approach, where catheter ablation of AF based on low-voltage areas in the left atrium improved clinical outcomes (65). Left atrial voltage maps were created in sinus rhythm after circumferential PVI, and low-voltage areas defined to regions with bipolar endocardial voltages of $<0.5\text{mV}$ (66). An ablation strategy was adopted with the aim of preventing substrate-based initiation and perpetuation by elimination of all reduced potentials of smaller areas, or by applying strategic linear lesions through larger low-voltage zones.

One of the limitations of voltage guided ablation strategies is the paucity of data to support the use of a bipolar 0.5mV cut off as a surrogate for scar with modern multi-electrode catheters used in EAM systems (67). This voltage threshold was based on data acquired in older studies using mostly ablation catheters in ventricular mapping studies. Recording electrode size, interelectrode spacing, tissue contact, mapping density and bipole orientation are all important determinants of voltage recordings and vary significantly with multi-electrode catheters (67–69). As such the threshold amplitude of 0.5mV for scar may itself need to be redefined, especially in the atrium.

4.1.3 Correlation of AF voltage maps with scar on MRI

Late-gadolinium cardiac magnetic resonance imaging (LGE-CMRI) has now been used to detect atrial fibrosis. The burden of atrial fibrosis as determined by LGE-CMRI positively correlates with clinical indices of atrial structural re-modelling and outcomes of catheter

ablation (70), and with the number of sites exhibiting high rotor activity using non-invasive mapping, and rotor trajectories showed a clustering around borders of fibrotic areas (71).

We recently described a novel technique on assessment of the atrial substrate with the use of AF voltage (72). Given that variable electrograms recorded during AF are generated by the dynamic interaction of local electrophysiology in response to the underlying myocardial architecture, we reported that, under conditions of adequate sampling duration of at least 4s, the spatial distribution of mean AF voltage is reproducible, and correlates with scar maps from LGE-CMRI (**Figure 6**). Mean AF voltage holds promise as a unique marker reflecting the functional response to the underlying AF substrate.

4.2 Mapping complex fractionated atrial electrograms (CFAEs)

In addition to representing local activation, the content of a clinical electrogram in itself has been hypothesised to contain information in regards to the underlying fibrillatory substrate and mechanism. Konings *et al* first described the complex fractionated atrial electrogram (CFAE) morphology in intraoperative studies in 1997 and from local activations maps demonstrated that they were representative of lines of conduction block, wavefront collisions, slowed conduction and pivot points for microreentrant circuits (73). CFAEs are defined as low voltage atrial electrograms (ranging from 0.04 to 0.25 mV) that have fractionation consisting of two deflections or more, and/or consist of a prolonged activation complexes with perturbation of the baseline with continuous deflections. They may be associated with a short cycle length (<120ms), form discrete complexes or fail to demonstrate isoelectric intervals between complexes (74).

4.2.1 Mapping and ablating CFAEs

Nademanee *et al* (2003) were first to create EAM of CFAE in AF and by applying radiofrequency ablation to areas with CFAEs managed to terminate AF in 95% of their patient group, consisting of both persistent and paroxysmal AF, and achieved a remarkable 91% arrhythmia free survival at one year follow up (75). Subsequent trials have failed to show such favourable results (76)(77).

The variable clinical outcomes have been attributed to a number of factors. CFAE mapping and ablation is performed in a very heterogeneous manner between different centres and there is a large degree of variance in inter-operator experience and targeting of CFAEs (78). The commercially available automated EAM systems, namely NavX and CARTO, vary significantly in how their algorithms classify CFAEs and currently expert consensus on how CFAEs should be mapped is lacking (79). Lastly, from a mechanistic point of view there is an argument that CFAEs are non-specific markers. Whilst they may take part in AF mechanisms, they can also be generated passively by mechanisms that do not contribute to AF (80). Classification of CFAEs by mapping local refractoriness of atrial tissue has demonstrated that the majority of the CFAE may in fact be far field signals and the rest may represent rapid localized AF site, AF acceleration dependent CFAEs or localized disorganization (81). At present, lack of specificity of CFAE is a concern and analytical tools for identifying true CFAEs contributing to AF mechanisms are lacking.

5. Novel tools for fibrillation analysis

In addition to mapping putative drivers and substrate, novel tools are being developed to provide unique mechanistic insight into fibrillatory mechanisms. There is increasing evidence

that drivers may in fact represent microreentrant circuits (82), and we recently describe a method we developed to map the nature of such circuits during fibrillation (83).

5.1 Algorithm for identification of lines of conduction block in microreentrant circuits

One of the challenges of processing fibrillatory data, particularly at the microscopic scale, is to isolate features of interest so that they may be studied in relation to specific hypotheses. To analyze our recordings of rotational activity at single-cell level, we developed an algorithm to highlight areas of consistent conduction block or slowing over the course of the recording.

This allowed us to generate ‘heat-maps’ of conduction block which can be studied in relation to features of the underlying substrate, such as cell size, ion channel density or gap-junctional coupling.

A pictorial outline of the algorithm is shown in [Figure 7](#). Firstly, each raw recording is processed using conventional techniques: spatial binning, temporal filtering and drift correction to reduce unwanted noise while retaining the underlying signal (36). A series of activation maps are generated for the range of time points in the recording, each covering a single rotation of the circuit.

Areas of high activation time disparity are then mapped ([Figure 7A](#)). For every pixel (i), neighbourhood pixels within a user-defined radius are found. For each neighbourhood pixel (j), the absolute activation time difference is calculated as $AT_{diff} = |AT_i - AT_j|$. This value is added to a running total at the geometric midpoint between i and j. After the values for every j have been calculated, the algorithm iterates onto the next i pixel in the activation map

and the process repeats. After the whole activation map has been processed, the mean activation time difference at each pixel is then calculated to generate a heatmap which highlights pixels between regions of large activation time differences. This generally corresponds to the wavefront itself and the core (as shown in [Figure 7B](#)).

The process is repeated for all activation maps in the recording, and the mean values through time calculated for each pixel. This has the effect of retaining only ‘constant’ features in the recordings (i.e. stable core) and eliminating features that change from frame to frame (i.e. the wavefront of activation). These maps have revealed that cores of rotational activations at microscopic level can be composed of *lines* of conduction block or slowing up to a size of $\sim 1.5\text{mm}$, rather than propagation occurring around a single point.

This map can be aligned and overlaid on further microscopy images to correlate the core of rotation with features to test specific hypotheses. As an example, we show in [Figure 7C](#) the core heatmap overlaid on fluorescently labelled wheat germ agglutinin membrane staining to study the effect of differences in 2D cell size to the location and morphology of the core. Zoomed portions of the full image show the level of detail we are able to achieve with this approach.

Using this technique, we recently demonstrated existence of rotational activity at a cellular scale (83). We studied features of the core of the rotational activation at single-cell level resolution ($2.6\mu\text{m}/\text{pixel}$) in a homogeneous substrate (2D monolayers of the HL1-6 cell line (25)(84)) using fluorescence microscopy. We observed rotational activity that remains stable for periods of several minutes despite the homogeneity of the substrate, and rotates around a

core that does not show the features of a phase singularity (when imaged with both Ca²⁺ and voltage sensitive dyes) (83). Our conduction delay algorithm showed that the cores of rotational drivers in HL1-6 cell line consist of areas with lines of conduction block. These data suggest that the rotational activity is sustained by micro-reentrant circuits, and not by functional reentry or spiral waves. Other conventional methods such as phase mapping would merely assign a phase singularity to the core of the rotational driver and not be able to distinguish between micro-reentry, functional reentry and spiral waves at the cellular level.

6. Conclusion

Analysis of myocardial fibrillation data presents a major challenge. Analytical techniques exist to map putative drivers of fibrillation or to map the underlying myocardial substrate sustaining fibrillation, and data analysed using these techniques, especially in the experimental laboratory, have provided important insights into the mechanisms of AF and VF. Nonetheless, many of these techniques can be limited by the resolution of the mapping data, especially in the clinical setting, and the success rates of therapeutic ablative approaches reliant on these techniques remain modest. There remains an urgent need to develop novel analytical tools to process myocardial fibrillation data.

Funding

The work is funded by the British Heart Foundation (grants number RG/16/3/32175, PG/15/59/31621 and PG/16/17/32069, and British Heart Foundation Centre of Research Excellence Studentships RE/13/4/30184), the Wellcome/EPSRC Centre for Medical Engineering (WT 203148/Z/16/Z), the Imperial College Centre for Cardiac Engineering and the National Institute for Health Research Imperial Biomedical Research Centre.

References

1. Pandit S V., Jalife J. Rotors and the dynamics of cardiac fibrillation. *Circ Res.* 2013;112(5):849–62.
2. Kim YH, Garfinkel A, Ikeda T, Wu TJ, Athill CA, Weiss JN, et al. Spatiotemporal complexity of ventricular fibrillation revealed by tissue mass reduction in isolated swine right ventricle: Further evidence for the quasiperiodic route to chaos hypothesis. *J Clin Invest.* 1997;100(10):2486–500.
3. Efimov IR, Nikolski VP, Salama G. Optical Imaging of the Heart. *Circ Res.* 2004 Jul 9;95(1):21 LP-33.
4. Barbhayia CR, Kumar S, Michaud GF. Mapping Atrial Fibrillation: 2015 Update. *J Atr Fibrillation.* 2015 Dec 31;8(4):1227.
5. J Shah A, Hocini M, Pascale P, Roten L, Komatsu Y, Daly M, et al. Body Surface Electrocardiographic Mapping for Non-invasive Identification of Arrhythmic Sources. *Arrhythmia Electrophysiol Rev.* 2013 Apr;2(1):16–22.
6. Rothberger CJ WH. Vorhofflimmern und Arrhythmia perpetua. *Wiener Klin Wochenschrift* , 1909, vol 22 (pg 839-844. 1909;22:839–44.
7. Moe GK, Rheinboldt WC, Abildskov JA. A computer model of atrial fibrillation. *Am Heart J.* 1964;67(2):200–20.
8. Allesie MA, Lammers WJEP, Bonke FIM HJ. Experimental evaluation of Moe's wavelet hypothesis of atrial fibrillation. Zipes DP JJ, editor. Orlando, Fla: WB Saunders; 1985. 265-275 p.
9. Davidenko JM, Pertsov A V, Salomonsz R, Baxter W, Jalife J. Stationary and drifting spiral waves of excitation in isolated cardiac muscle. *Nature.* 1992 Jan 23;355:349.

10. Verheule S, Eckstein J, Linz D, Maesen B, Bidar E, Gharaviri A, et al. Role of endo-epicardial dissociation of electrical activity and transmural conduction in the development of persistent atrial fibrillation. *Prog Biophys Mol Biol*. 2014 Aug;115(2–3):173–85.
11. Witkowski FX, Leon LJ, Penkoske PA, Giles WR, Spano ML, Ditto WL, et al. Spatiotemporal evolution of ventricular fibrillation. *Nature*. 1998 Mar;392(6671):78–82.
12. Garfinkel A, Chen PS, Walter DO, Karagueuzian HS, Kogan B, Evans SJ, et al. Quasiperiodicity and chaos in cardiac fibrillation. *J Clin Invest*. 1997 Jan;99(2):305–14.
13. Bradley CP, Clayton RH, Nash MP, Mourad A, Hayward M, Paterson DJ, et al. Human ventricular fibrillation during global ischemia and reperfusion: paradoxical changes in activation rate and wavefront complexity. *Circ Arrhythm Electrophysiol*. 2011 Oct;4(5):684–91.
14. Zaitsev A V, Guha PK, Sarmast F, Kolli A, Berenfeld O, Pertsov AM, et al. Wavebreak formation during ventricular fibrillation in the isolated, regionally ischemic pig heart. *Circ Res*. 2003 Mar;92(5):546–53.
15. Vidmar D, Krummen DE, Hayase J, Narayan SM, Ho G, Rappel W-J. Spatiotemporal Progression of Early Human Ventricular Fibrillation. *JACC Clin Electrophysiol*. 2017 Dec;3(12):1437–46.
16. Nair K, Umapathy K, Farid T, Masse S, Mueller E, Sivanandan R V, et al. Intramural Activation During Early Human Ventricular Fibrillation. *Circ Arrhythmia Electrophysiol*. 2011 Oct 1;4(5):692 LP-703.
17. Krummen DE, Hayase J, Morris DJ, Ho J, Smetak MR, Clopton P, et al. Rotor stability

- separates sustained ventricular fibrillation from self-terminating episodes in humans. *J Am Coll Cardiol*. 2014 Jun;63(24):2712–21.
18. Latchamsetty R, Kocheril AG. Review of Dominant Frequency Analysis in Atrial Fibrillation. *J Atr Fibrillation*. 2009 Oct 1;2(3):204.
 19. Sanders P, Berenfeld O, Hocini M, Jaïs P, Vaidyanathan R, Hsu L-F, et al. Spectral Analysis Identifies Sites of High-Frequency Activity Maintaining Atrial Fibrillation in Humans. *Circulation*. 2005 Aug 9;112(6):789 LP-797.
 20. Rodrigo M, Climent AM, Liberos A, Fernández-Avilés F, Berenfeld O, Atienza F, et al. Highest dominant frequency and rotor positions are robust markers of driver location during noninvasive mapping of atrial fibrillation: A computational study. *Hear Rhythm*. 2017 Aug 26;14(8):1224–33.
 21. Hwang M, Song JS, Lee YS, Li C, Shim EB, Pak HN. Electrophysiological rotor ablation in in-silico modeling of atrial fibrillation: Comparisons with dominant frequency, shannon entropy, and phase singularity. *PLoS One*. 2016;11(2):1–15.
 22. Atienza F, Almendral J, Ormaetxe JM, Moya Á, Martínez-Alday JD, Hernández-Madrid A, et al. Comparison of radiofrequency catheter ablation of drivers and circumferential pulmonary vein isolation in atrial fibrillation: A noninferiority randomized multicenter RADAR-AF trial. *J Am Coll Cardiol*. 2014;64(23):2455–67.
 23. Atienza F, Almendral J, Jalife J, Zlochiver S, Ploutz-Snyder R, Torrecilla EG, et al. Real-time dominant frequency mapping and ablation of dominant frequency sites in atrial fibrillation with left-to-right frequency gradients predicts long-term maintenance of sinus rhythm. *Hear Rhythm*. 2009 Jan 6;6(1):33–40.
 24. Jarman JWE, Wong T, Kojodjojo P, Spohr H, Davies JER, Roughton M, et al. Organizational index mapping to identify focal sources during persistent atrial

- fibrillation. *J Cardiovasc Electrophysiol*. 2014;25(4):355–63.
25. Salinet J, Schlindwein FS, Stafford P, Almeida TP, Li X, Vanheusden FJ, et al. Propagation of meandering rotors surrounded by areas of high dominant frequency in persistent atrial fibrillation. *Heart Rhythm*. 2017;14(9):1269–78.
 26. Annoni EM, Arunachalam SP, Kapa S, Mulpuru SK, Friedman PA, Tolkacheva EG. Novel quantitative analytical approaches for rotor identification and associated implications for mapping. *IEEE Trans Biomed Eng*. 2018;65(2):273–81.
 27. Ganesan AN, Kuklik P, Lau DH, Brooks AG, Baumert M, Lim WW, et al. Bipolar electrogram Shannon entropy at sites of rotational activation implications for ablation of atrial fibrillation. *Circ Arrhythmia Electrophysiol*. 2013;6(1):48–57.
 28. Arunachalam SP, Mulpuru SK, Friedman PA, Tolkacheva EG. Feasibility of visualizing higher regions of Shannon entropy in atrial fibrillation patients. *Proc Annu Int Conf IEEE Eng Med Biol Soc EMBS*. 2015;2015–Novem:4499–502.
 29. Nattel S, Xiong F, Aguilar M. Demystifying rotors and their place in clinical translation of atrial fibrillation mechanisms. *Nat Rev Cardiol*. 2017 Apr 6;14:509.
 30. Narayan SM, Krummen DE, Shivkumar K, Clopton P, Rappel W-J, Miller JM. Treatment of Atrial Fibrillation by the Ablation of Localized Sources. *J Am Coll Cardiol*. 2012 Aug 14;60(7):628 LP-636.
 31. Gianni C, Mohanty S, Di Biase L, Metz T, Trivedi C, Gokoglan Y, et al. Acute and early outcomes of focal impulse and rotor modulation (FIRM)-guided rotors-only ablation in patients with nonparoxysmal atrial fibrillation. *Heart Rhythm*. 2016 Apr; 13(4):830–5.
 32. Balouch M, Gucuk Ipek E, Chrispin J, Bajwa RJ, Zghaib T, Berger RD, et al. Impact of rotor temperospatial stability on acute and one-year atrial fibrillation ablation

- outcomes. *Clin Cardiol*. 2017 Jun;40(6):383–9.
33. Steinberg JS, Shah Y, Bhatt A, Sichrovsky T, Arshad A, Hansinger E, et al. Focal impulse and rotor modulation: Acute procedural observations and extended clinical follow-up. *Heart Rhythm*. 2017 Feb 1;14(2):192–7.
 34. Rosenbaum D, Jalife J. Spatial and temporal organization during cardiac fibrillation. Futur Publ Company, New York. 2001 Mar 5;33:46:75.
 35. Umapathy K, Nair K, Masse S, Krishnan S, Rogers J, Nash MP, et al. Phase Mapping of Cardiac Fibrillation. *Circ Arrhythmia Electrophysiol*. 2010 Feb 1;3(1):105 LP-114.
 36. Laughner JI, Ng FS, Sulkin MS, Arthur RM, Efimov IR. Processing and analysis of cardiac optical mapping data obtained with potentiometric dyes. *Am J Physiol Heart Circ Physiol*. 2012 Oct;303(7):H753-65.
 37. Bray M-A, Wikswo JP. Considerations in phase plane analysis for nonstationary reentrant cardiac behavior. *Phys Rev E*. 2002 May 2;65(5):51902.
 38. Iyer AN, Gray RA. An Experimentalist's Approach to Accurate Localization of Phase Singularities during Reentry. *Ann Biomed Eng*. 2001 Jan;29(1):47–59.
 39. Gray RA, Jalife J. Video imaging of cardiac fibrillation. In: Rosenbaum D, Jalife J, editors. *Optical Mapping of Cardiac Excitation and Arrhythmias*. New York: Futura Publishing Company; 2001. p. 245–56.
 40. Kuklik P, Zeemering S, Maesen B, Maessen J, Crijns HJ, Verheule S, et al. Reconstruction of Instantaneous Phase of Unipolar Atrial Contact Electrogram Using a Concept of Sinusoidal Recomposition and Hilbert Transform. *IEEE Trans Biomed Eng*. 2015;62(1):296–302.
 41. Nash MP, Mourad A, Clayton RH, Sutton PM, Bradley CP, Hayward M, et al. Evidence for Multiple Mechanisms in Human Ventricular Fibrillation. *Circulation*.

- 2006 Aug 8;114(6):536 LP-542.
42. Rogers JM. Combined phase singularity and wavefront analysis for optical maps of ventricular fibrillation. *IEEE Trans Biomed Eng.* 2004;51(1):56–65.
 43. Bray MA, Wikswo JP. Use of topological charge to determine filament location and dynamics in a numerical model of scroll wave activity. *IEEE Trans Biomed Eng.* 2002;49(10):1086–93.
 44. Pathik B, Kalman JM, Walters T, Kuklik P, Zhao J, Madry A, et al. Transient Rotor Activity During Prolonged 3-Dimensional Phase Mapping in Human Persistent Atrial Fibrillation. *JACC Clin Electrophysiol.* 2018;4(1):72–83.
 45. Haissaguerre M, Hocini M, Denis A, Shah AJ, Komatsu Y, Yamashita S, et al. Driver domains in persistent atrial fibrillation. *Circulation.* 2014 Aug;130(7):530–8.
 46. Roney CH, Cantwell CD, Qureshi NA, Chowdhury RA, Dupont E, Lim PB, et al. Rotor Tracking Using Phase of Electrograms Recorded During Atrial Fibrillation. *Ann Biomed Eng.* 2017 Apr;45(4):910–23.
 47. Child N, Clayton RH, Roney CR, Laughner JJ, Shuros A, Neuzil P, et al. Unraveling the Underlying Arrhythmia Mechanism in Persistent Atrial Fibrillation. *Circ Arrhythmia Electrophysiol.* 2018 Jun 1;11(6).
 48. Vijayakumar R, Vasireddi SK, Cuculich PS, Faddis MN, Rudy Y. Methodology Considerations in Phase Mapping of Human Cardiac Arrhythmias. *Circ Arrhythm Electrophysiol.* 2016 Nov;9(11).
 49. Rodrigo M, Climent AM, Liberos A, Fernandez-Aviles F, Berenfeld O, Atienza F, et al. Technical Considerations on Phase Mapping for Identification of Atrial Reentrant Activity in Direct- and Inverse-Computed Electrograms. *Circ Arrhythm Electrophysiol.* 2017 Sep;10(9).

50. Roney CH, Cantwell CD, Bayer JD, Qureshi NA, Lim PB, Tweedy JH, et al. Spatial Resolution Requirements for Accurate Identification of Drivers of Atrial Fibrillation. *Circ Arrhythmia Electrophysiol*. 2017 May 1;10(5):e004899.
51. Aronis KN, Ashikaga H. Impact of number of co-existing rotors and inter-electrode distance on accuracy of rotor localization. *J Electrocardiol*. 2018 Jan;51(1):82–91.
52. Jacquemet V. A statistical model of false negative and false positive detection of phase singularities. *Chaos An Interdiscip J Nonlinear Sci*. 2017 Oct;27(10):103124.
53. Parameswaran R, Voskoboinik A, Gorelik A, Lee G, Kistler PM, Sanders P, et al. Clinical impact of rotor ablation in atrial fibrillation: a systematic review. *EP Eur*. 2018 Jan 11;eux370-eux370.
54. Hutchinson MD, Gerstenfeld EP, Desjardins B, Bala R, Riley MP, Garcia FC, et al. Endocardial Unipolar Voltage Mapping to Detect Epicardial VT Substrate in Patients with Nonischemic Left Ventricular Cardiomyopathy. *Circ Arrhythm Electrophysiol*. 2011 Feb 1;4(1):49–55.
55. Verma A, Wazni OM, Marrouche NF, Martin DO, Kilicaslan F, Minor S, et al. Pre-existent left atrial scarring in patients undergoing pulmonary vein antrum isolation: An independent predictor of procedural failure. *J Am Coll Cardiol*. 2005;45(2):285–92.
56. Ghoraani B, Dalvi R, Gizurason S, Das M, Ha A, Suszko A, et al. Localized rotational activation in the left atrium during human atrial fibrillation: Relationship to complex fractionated atrial electrograms and low-voltage zones. *Hear Rhythm*. 2013;10(12):1830–8.
57. Koutalas E, Rolf S, Dinov B, Richter S, Arya A, Bollmann A, et al. Contemporary Mapping Techniques of Complex Cardiac Arrhythmias – Identifying and Modifying the Arrhythmogenic Substrate. *Arrhythmia Electrophysiol Rev*. 2015 May 10;4(1):19–

- 27.
58. De Groot NMS, Schalij MJ, Zeppenfeld K, Blom NA, Van der Velde ET, Van der Wall EE. Voltage and Activation Mapping: How the Recording Technique Affects the Outcome of Catheter Ablation Procedures in Patients With Congenital Heart Disease. *Circulation*. 2003;108(17):2099–106.
59. Masuda M, Fujita M, Iida O, Okamoto S, Ishihara T, Nanto K, et al. Comparison of Left Atrial Voltage between Sinus Rhythm and Atrial Fibrillation in Association with Electrogram Waveform. *Pacing Clin Electrophysiol*. 2017 May;40(5):559–67.
60. Rudy Y, Quan WL. A model study of the effects of the discrete cellular structure on electrical propagation in cardiac tissue. *Circ Res*. 1987 Dec 1;61(6):815 LP-823.
61. Cabo C, Pertsov AM, Baxter WT, Davidenko JM, Gray RA, Jalife J. Wave-front curvature as a cause of slow conduction and block in isolated cardiac muscle. *Circ Res*. 1994 Dec 1;75(6):1014 LP-1028.
62. Teh AW, Kistler PM, Lee G, Medi C, Heck PM, Spence SJ, et al. Electroanatomic remodeling of the left atrium in paroxysmal and persistent atrial fibrillation patients without structural heart disease. *J Cardiovasc Electrophysiol*. 2012 Mar;23(3):232–8.
63. Fiala M, Wichterle D, Chovancik J, Bulkova V, Wojnarova D, Nevralova R, et al. Left Atrial Voltage during Atrial Fibrillation in Paroxysmal and Persistent Atrial Fibrillation Patients. *Pacing Clin Electrophysiol*. 2009;33(5):541–8.
64. Di Biase L, Santangeli P, Burkhardt DJ, Bai R, Mohanty P, Carbucicchio C, et al. Endo-Epicardial Homogenization of the Scar Versus Limited Substrate Ablation for the Treatment of Electrical Storms in Patients With Ischemic Cardiomyopathy. *J Am Coll Cardiol*. 2012;60(2):132–41.
65. Rolf S, Kircher S, Arya A, Eitel C, Sommer P, Richter S, et al. Tailored Atrial

- Substrate Modification Based on Low-Voltage Areas in Catheter Ablation of Atrial Fibrillation. *Circ Arrhythmia Electrophysiol.* 2014 Oct 1;7(5):825 LP-833.
66. Marcus GM, Yang Y, Varosy PD, Ordovas K, Tseng ZH, Badhwar N, et al. Regional left atrial voltage in patients with atrial fibrillation. *Heart Rhythm.* 2007;4(2):138–44.
 67. Anter E, Josephson ME. Bipolar voltage amplitude: What does it really mean? *Heart Rhythm.* 2016 Jan 1;13(1):326–7.
 68. Anter E, Tschabrunn CM, Josephson ME. High-resolution mapping of scar-related atrial arrhythmias using smaller electrodes with closer interelectrode spacing. *Circ Arrhythm Electrophysiol.* 2015 Jun;8(3):537–45.
 69. Haldar SK, Magtibay K, Porta-Sanchez A, Massé S, Mitsakakis N, Lai PFH, et al. Resolving bipolar electrogram voltages during atrial fibrillation using omnipolar mapping. *Circ Arrhythmia Electrophysiol.* 2017;10(9).
 70. Akoum N, Wilber D, Hindricks G, Jais P, Cates J, Marchlinski F, et al. MRI Assessment of Ablation-Induced Scarring in Atrial Fibrillation: Analysis from the DECAAF Study. *J Cardiovasc Electrophysiol.* 2015 May;26(5):473–80.
 71. Clement-Guinaudeau S, Montaudon M, Laurent F, Jais P, Cochet H. Atrial late gadolinium enhancement on MRI relates to the electrophysiological substrate of persistent atrial fibrillation. *J Cardiovasc Magn Reson.* 2015;17(1):O22.
 72. Qureshi N, Doherty D, Kim S, Bai W, Matthew S-S, Ng FS, et al. 18-06: AF Voltage as a Functional Marker for Atrial Fibrosis: Assessing the spatio-temporal correlation of low voltage regions during AF vs SR with late-gadolinium enhanced CMRI defined fibrosis in patients with persistent AF. Vol. 18, *EP Europace.* 2016. 164-164 p.
 73. Konings KT, Smeets JL, Penn OC, Wellens HJ, Allessie MA. Configuration of unipolar atrial electrograms during electrically induced atrial fibrillation in humans.

- Circulation. 1997 Mar;95(5):1231–41.
74. Nademanee K, Lockwood E, Oketani N, Gidney B. Catheter ablation of atrial fibrillation guided by complex fractionated atrial electrogram mapping of atrial fibrillation substrate. *J Cardiol*. 2010;55(1):1–12.
 75. Nademanee K, McKenzie J, Kosar E, Schwab M, Sunsaneewitayakul B, Vasavakul T, et al. A new approach for catheter ablation of atrial fibrillation: mapping of the electrophysiologic substrate. *J Am Coll Cardiol*. 2004 Jun;43(11):2044–53.
 76. Chen M, Yang B, Chen H, Ju W, Zhang F, Tse H-F, et al. Randomized comparison between pulmonary vein antral isolation versus complex fractionated electrogram ablation for paroxysmal atrial fibrillation. *J Cardiovasc Electrophysiol*. 2011 Sep; 22(9):973–81.
 77. Verma A, Jiang C, Betts TR, Chen J, Deisenhofer I, Mantovan R, et al. Approaches to Catheter Ablation for Persistent Atrial Fibrillation. *N Engl J Med*. 2015;372(19):1812–22.
 78. Scherr D, Dalal D, Cheema A, Cheng A, Henrikson CA, Spragg D, et al. Automated detection and characterization of complex fractionated atrial electrograms in human left atrium during atrial fibrillation. *Hear Rhythm*. 2007;4(8):1013–20.
 79. Lau DH, Maesen B, Zeemering S, Kuklik P, van Hunnik A, Lankveld TAR, et al. Indices of bipolar complex fractionated atrial electrograms correlate poorly with each other and atrial fibrillation substrate complexity. *Hear Rhythm*. 2015 Jul;12(7):1415–23.
 80. Providência R, Lambiase PD, Srinivasan N, Ganesha Babu G, Bronis K, Ahsan S, et al. Is There Still a Role for CFAE Ablation in Addition to Pulmonary Vein Isolation in Patients with Paroxysmal and Persistent Atrial Fibrillation? A Meta-Analysis of 1,415

- Patients. *Circ Arrhythmia Electrophysiol*. 2015 Jun 16;
81. Narayan SM, Wright M, Derval N, Jadidi A, Forclaz A, Nault I, et al. Classifying fractionated electrograms in human atrial fibrillation using monophasic action potentials and activation mapping: evidence for localized drivers, rate acceleration, and nonlocal signal etiologies. *Heart Rhythm*. 2011 Feb;8(2):244–53.
 82. Hansen BJ, Zhao J, Csepe TA, Moore BT, Li N, Jayne LA, et al. Atrial fibrillation driven by micro-anatomic intramural re-entry revealed by simultaneous sub-epicardial and sub-endocardial optical mapping in explanted human hearts. *Eur Heart J*. 2015 Sep 14;36(35):2390–401.
 83. Houston C, Tzortzis KN, Roney C, Saglietto A, Pitcher DS, Cantwell CD, et al. Characterisation of re-entrant circuit (or rotational activity) in vitro using the HL1-6 myocyte cell line. *J Mol Cell Cardiol*. 2018;119:155–64.
 84. Claycomb WC, Lanson NA, Stallworth BS, Egeland DB, Delcarpio JB, Bahinski A, et al. HL-1 cells: A cardiac muscle cell line that contracts and retains phenotypic characteristics of the adult cardiomyocyte. *Proc Natl Acad Sci*. 1998 Mar 17;95(6):2979 LP-2984.

Figure 1: Dominant Frequency Maps of VF: (A) Optical action potential data for two pixels during a recording of ventricular fibrillation in a langendorff perfused rat heart. (B) Dominant frequency map: frequency spectrum of both these pixels is shown (left) and the frequency with the largest power for each pixel is plotted on a colour map. The corresponding histogram of DF values for the entire heart is also shown (bottom right).

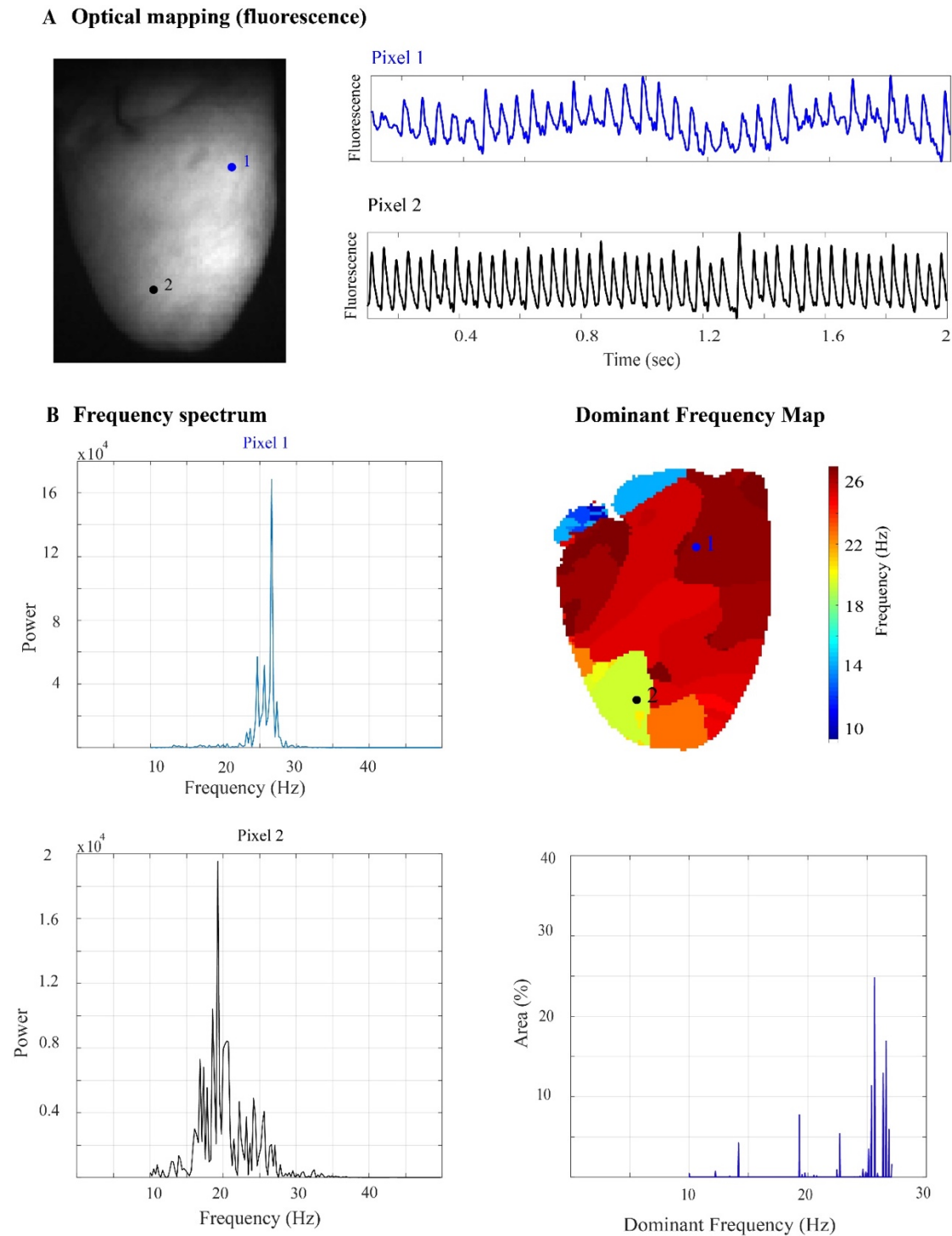


Figure 2: Shannon Entropy Maps of VF: The optical action potential data for the two pixels during a recording of ventricular fibrillation shown in Figure 1 was used to construct a Shannon entropy map. The fluorescence signal from optical mapping of each pixel is placed in fluorescence amplitude bins with frequency of occurrence over the recording period on the y axis (left), and the Shannon entropy of each pixel was calculated using the relative probability of the signal falling in each fluorescence amplitude bin. The Shannon entropy values for each pixel are then depicted on a Shannon entropy map (top right), the distribution of SE values shown on the histogram (bottom right).

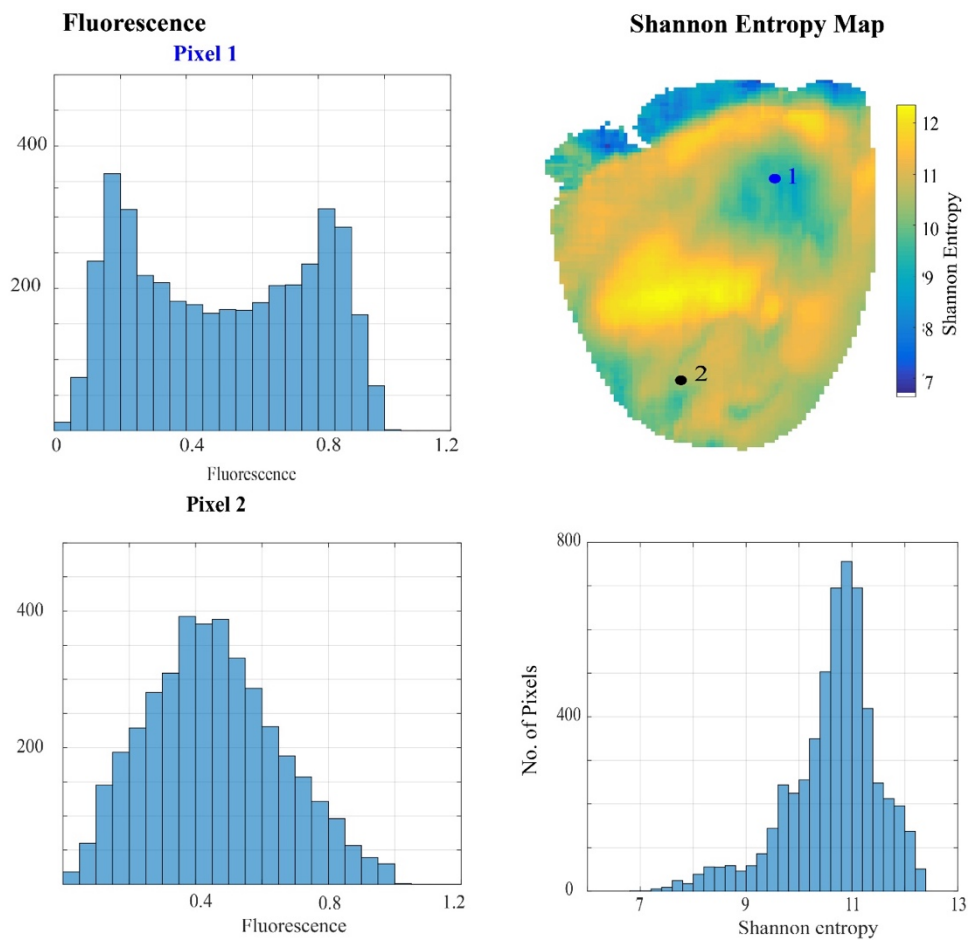


Figure 3. Calculating phase in optically mapped VF: (A-F) Steps for calculating the phase are as follow. **(A)** Tag minima (green circles) of the signal using a sliding window, then tag maxima (red circles) between each pair of minima, and finally remove any small amplitude pairs of maxima-minima. **(B)** Cubic spline fits were performed on the maxima and minima of the signal, and the average of these maxima (red) and minima (green) splines (the mean line, shown in black) was subtracted from the signal to give a signal of zero mean. **(C)** The real and imaginary parts of the Hilbert transform of this zero-mean signal were plotted in the phase plane. **(D)** The angle around the trajectory in (C) gives the phase angle. A phase map of ventricular fibrillation at a single time point is shown in **(E)**, and a phase singularity heat map can be used to show sites with high incidences phase singularities over time **(F)**.

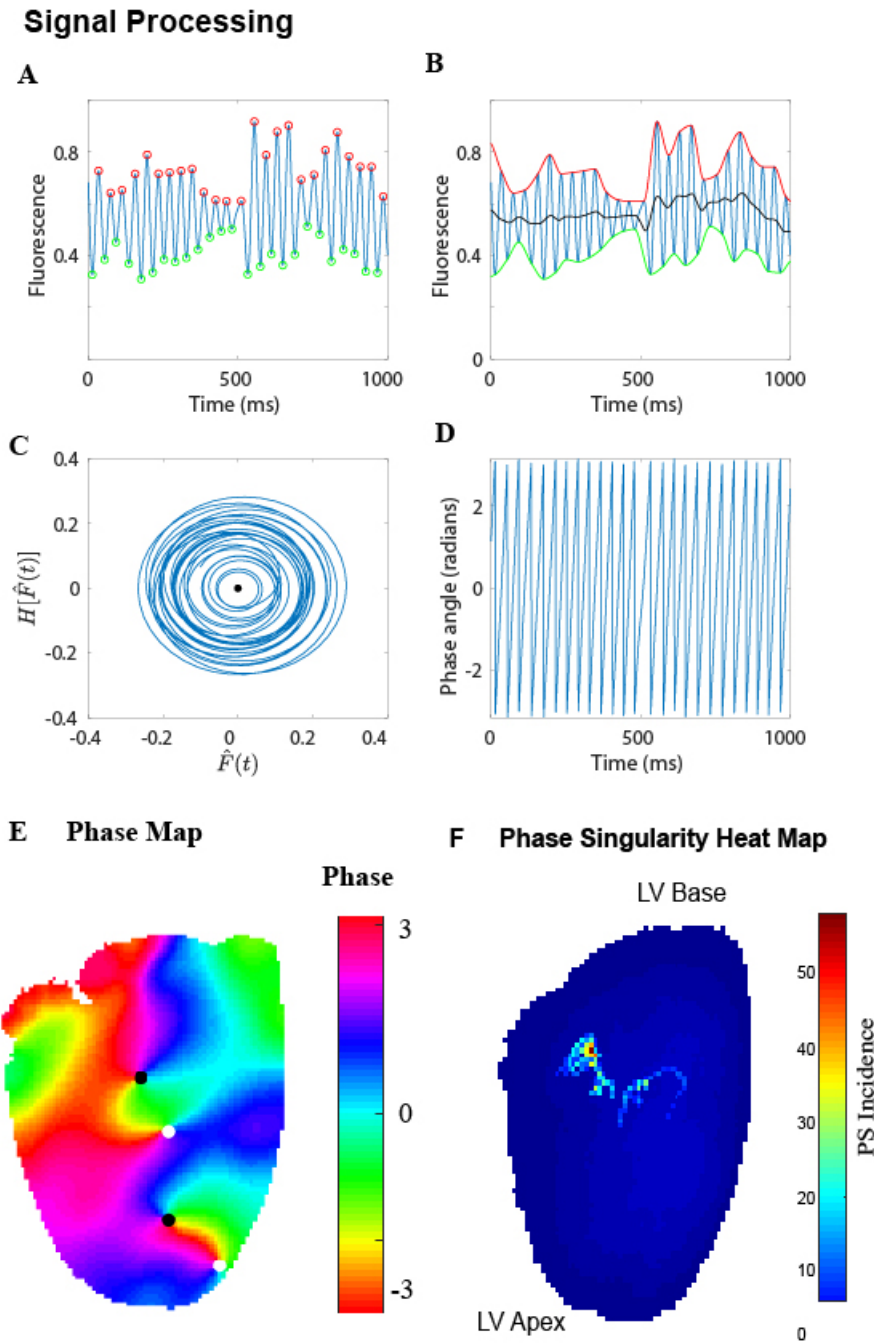


Figure 4. Outline of filtering and processing steps involved in phase calculation of unipolar and bipolar electrogram signals. Raw unipolar electrograms are pre-processed (**a–c**). Both unipolar electrogram derivatives and bipolar electrograms are then pre-processed (**d–f**) before tagging of individual activations (**g–h**). Phase is then calculated identically for both modalities of signal (**i–n**) to give unipolar and bipolar phase (**o–p**). [Figure reproduced from Roney et al. (46), in line with Creative Commons Attribution license (CC BY 4.0)].

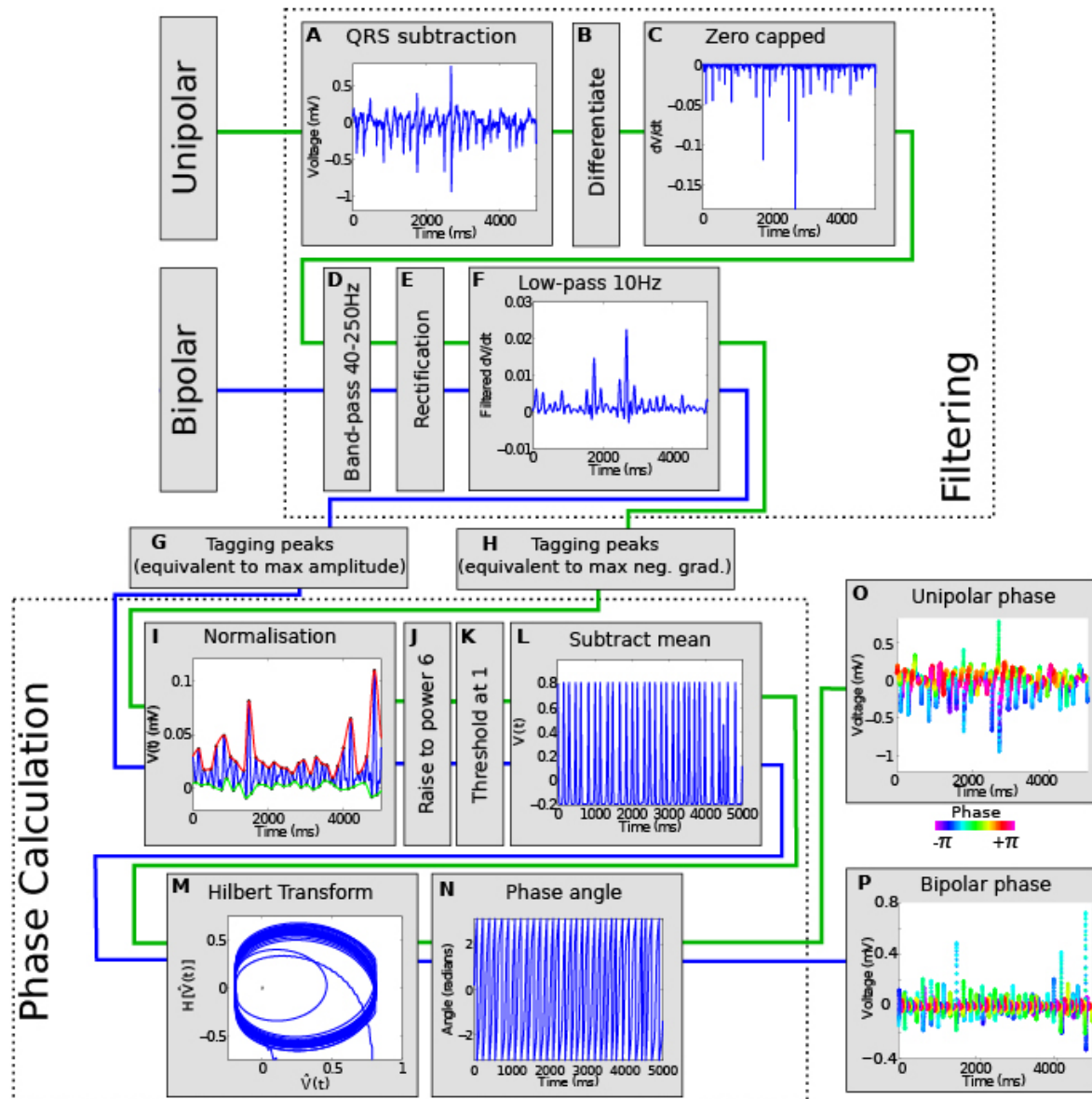


Figure 5. Left atrial 3D reconstruction showing phase singularity heat maps during AF. Regions of high and low phase singularity during AF are shown for three patients, with maps created using bipolar electrogram phase analysis. [Figure reproduced from Roney et al. (46), in line with Creative Commons Attribution license (CC BY 4.0)].

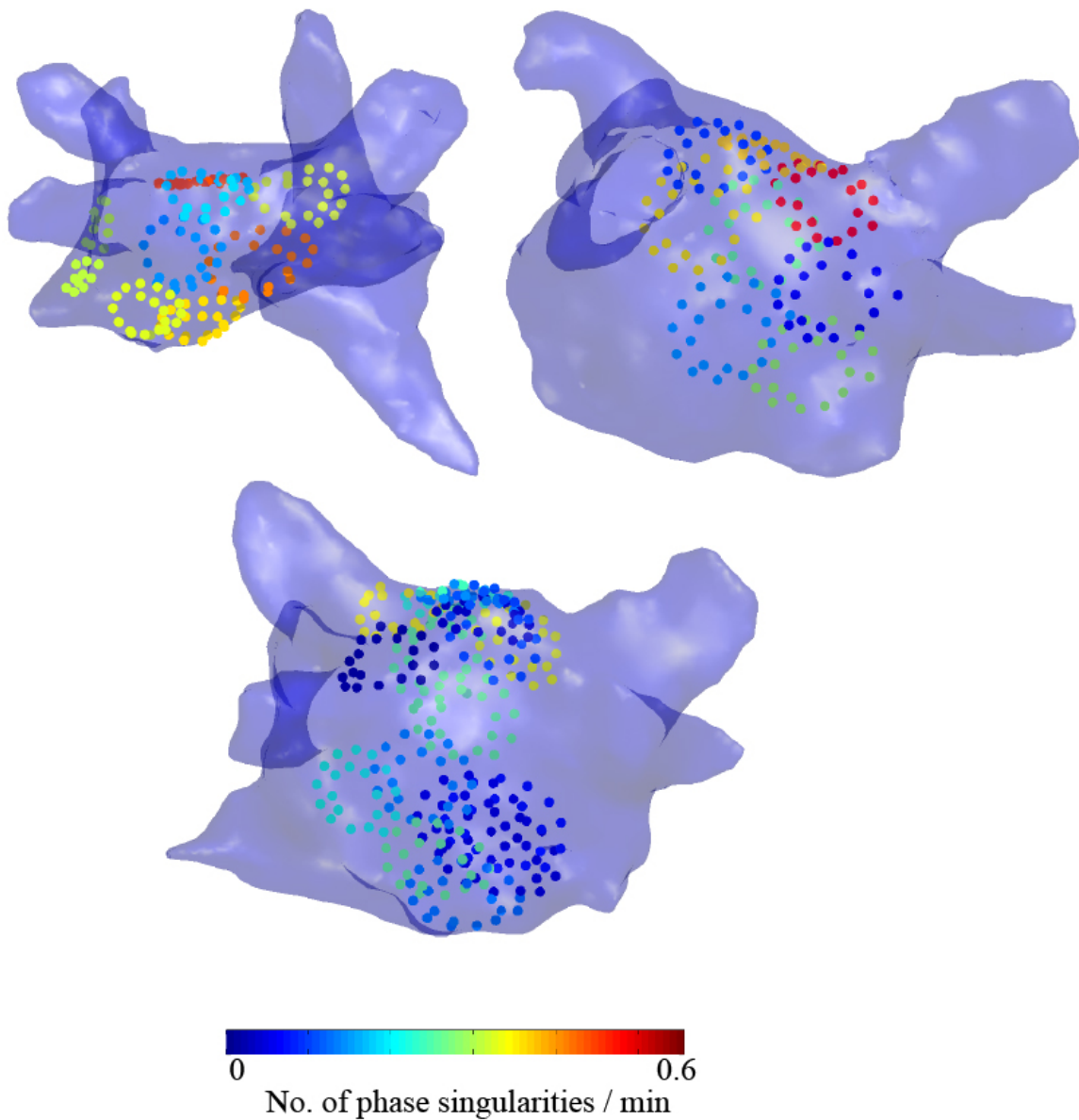


Figure 6. AF voltage maps correlate well with MRI scar maps. Electroanatomical voltage maps in AF (left), with their corresponding electrograms. The AF voltage maps were created using 8 second segments of recordings, and the maps represents the mean peak-to-peak AF voltage (AF-V) (on a research version of Ensite™ Velocity, SJM). The LGE-CMRI derived atrial scar maps (right) are imported, and registered to the left atrial geometries. This representative example illustrates good correlation between regions of low mean AF voltage and scar as defined by LGE-CMRI.

Voltage Map

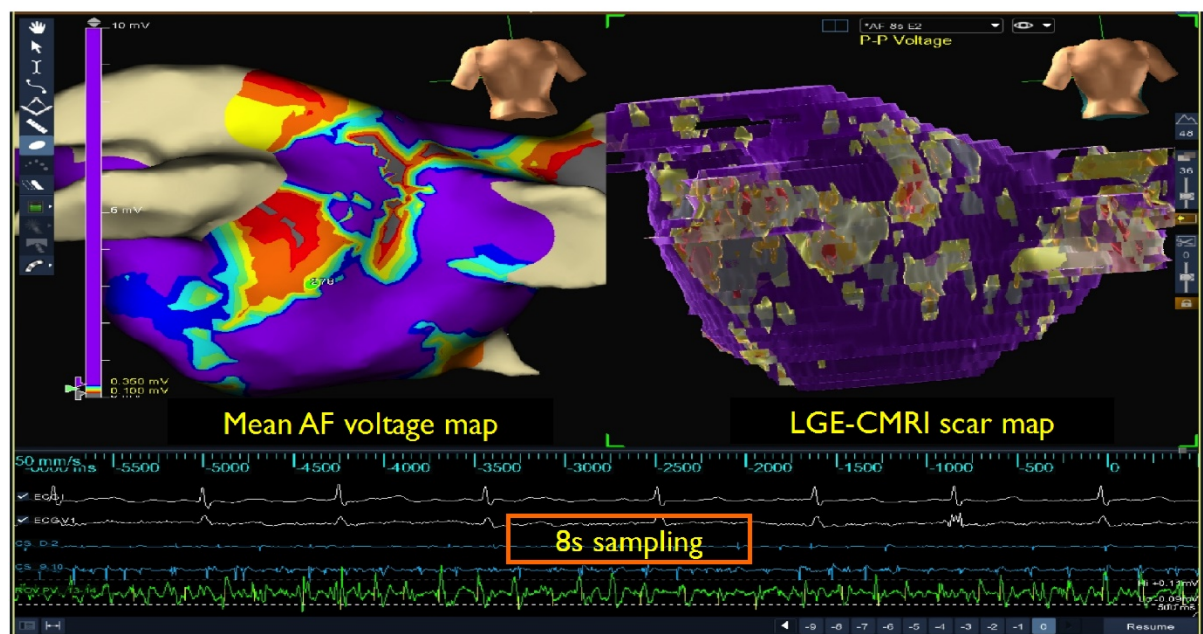


Figure 7. Processing and analysis of conduction block at single-cell level in HL1-6 myocyte monolayer. (A) Processing stage of algorithm: each pixel in the activation map is iterated through (first graphic). For each pixel, its neighbourhood is determined and then the absolute activation time difference between it and each neighbouring pixel determined (next two graphics). After repeating for all neighbourhood pixels for every pixel in the activation map, a heatmap highlighting areas of large activation differences is generated (last two graphics). (B) This process can be repeated for multiple activation maps generated from the same recording. When these heatmaps are summed and averaged, the resulting heatmap isolates the ‘constant’ features of the rotational activity. (C) The final heatmap can be overlaid on wheat germ agglutinin membrane staining to study the correlation between cell morphology, core shape and/or core location.

